ISBN: 978-3-95450-184-7 doi:10.18429/JACoW-IPAC2018-THXGBE2

OPTICAL DIAGNOSTICS FOR EXTREME BEAM CONDITIONS*

R.B. Fiorito†,1, University of Liverpool, Cockcroft Institute, WA44AD Daresbury, UK
[1]also at the University of Maryland, Institute for Research in Electronics and Applied Physics, 20742 College Park, USA

Abstract

The development of simple, fast, precise and robust beam diagnostics is absolutely necessary to optimize the performance of present accelerators and to satisfy the needs of future accelerators, in particular those with extreme properties such as high brightness FELs and plasma wake-field accelerators. This invited talk will present the underlying physics and results from simulation and experiments for a number of advanced optical beam diagnostics currently under development at various accelerator research laboratories including efforts at the Cockcroft Institute.

INTRODUCTION

I will refer to beams with rms size and transverse emittances $\sigma, \varepsilon \le 1\mu m$, divergences $\sigma' \le \mu rad$, bunch lengths $c\tau \le \mu m$, intensities $\chi \approx 1$ and measurable dynamic range, DR $>10^5$ as "extreme" conditions, in the sense that the types of optical diagnostics needed to measure these properties exceed the limits of those commonly used or available. Also I emphasize techniques that can be used for a wide range of beam conditions and accelerator platforms, are easily implemented, are minimally invasive to the beam and have the potential to measure the beam parameters of a single bunch. Space limitation demands that I cannot discuss in detail or even mention all of the novel techniques being investigated - there are far too many to include in a brief review paper. So I have selected a representative sample of techniques that meet the criteria mentioned above and have common threads.

Five types of recent diagnostic methods will be reviewed: 1) convolution and de-convolution of the so called 'single particle source function' (SPF), i.e. the theoretically calculable or simulated image formed by a single particle, to achieve an rms size from a measured beam image; 2) measurement of the visibility of beam images with rms widths less than or comparable to the width of the SPF to infer rms beam size; 2) use of the visibility of beam radiation *interferences* from two or more sources to infer the beam size and/or the beam divergence; 3) high dynamic range beam imaging with optical masks; 4) optical phase space mapping and emittance measurement methods applicable to high intensity beams; and 5) a novel bunch length diagnostic that utilizes the *spatial* rather than the spectral properties of coherent radiation produced by a charged particle bunch.

BEAM IMAGING USING THE SPF

OTR

The properties of optical transition radiation (OTR) from a single particle have been well studied theoretically, computationally and experimentally [1-4]. The SPF of OTR presented in Figure 1 (left), shows that the visibility, $V = I_{max}/I_{min}$, as well as the overall shape of the distribution can be used to measure transverse beam sizes that are smaller than the full width of the SPF [2], an idea that we will see is also being applied to other types of beam radiation.

Figure 1 (right) shows an empirical fit to a vertical scan of the measured OTR distribution from a highly focused electron beam generated at KEK's ATF2 accelerator. The measurements were done using a single achromat and a 40 nm band-pass filter. A vertical rms beam size $\sigma = 750nm$ was measured by fitting an empirical function to the OTR data [4]. The fit depends on the optical parameters of the imaging system as well as the beam size.

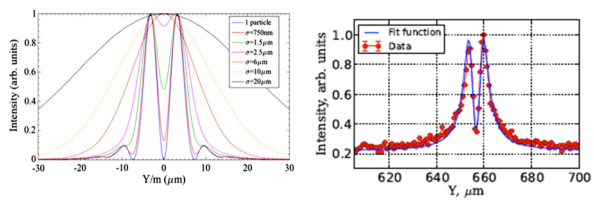

Figure 1: (left) OTR profiles resulting from a convolution of the SPF with Gaussian beam distributions; (right) empirical fit to measured vertical OTR profile.

The influence of band pass on these types of measurements has recently been investigated in detail [5]. It has been found that a larger band pass than previously realized can be used to improve the dynamic range and signal to noise ratio, while maintaining the sensitivity to beam size. Figure 2 (left) shows the percentage change in the visibility as a function of beam size for various bandwidths; (right) shows an enlarged view of the left hand corner of the left graph. Note that the change in visibility becomes smaller as the beam size decreases.

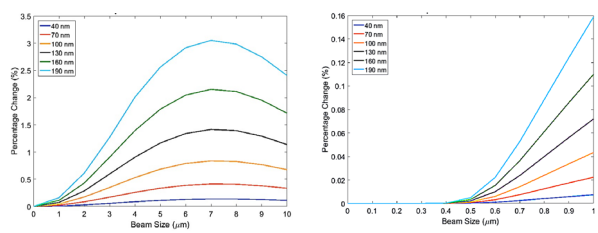

Figure 2: Effect of band pass on the OTR SPF visibility.

* Work supported by the European Research Commission
† ralph.fiorito@cockcroft.ac.uk; ralph.fiorito@ymail.com

ISBN: 978-3-95450-184-7 doi:10.18429/JACoW-IPAC2018-THXGBE2

A novel algorithm has been developed to retrieve the rms beam size using Zemax Optical Studio (ZOS) to take into account optical effects, e.g. chromatic and spherical aberrations and band pass. The input to the algorithm is the theoretically calculated OTR SPF, which depends only on the beam energy, the observed wavelength and the field of view of the lens. Since ZOS can only propagate the wave front for a single wavelength, a MATLAB code has been written that calls and loops ZOS through a band of wavelengths, taking into account the transmissivity of each wavelength in the filter band pass, to produce an integrated SPF. The code then performs a convolution of this function with a Gaussian beam profile and compares the calculated to the measured OTR distribution. The beam size is varied until the best fit is found.

In order to do the required calculations in a reasonable amount of time and maintain good spatial resolution for the input OTR SPF, a new technique has been developed. This method scales the energy down to a lower value if the beam energy is in the GeV or higher range, while maintaining a field of view, $\Theta \geq 10/\gamma$. As shown in Figure 3, this produces an almost energy independent SPF [5], which can be applied to higher energy beams and incorporated in the fitting algorithm.

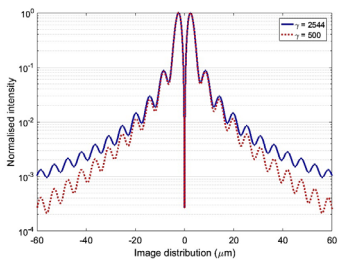

Figure 3: Comparison of the OTR SPFs from 250 and 1300 MeV electrons observed with an ideal lens.

OSR Filament Beam Spread Function

A technique to measure the beam that is similar to what has been done for OTR has been implemented at the Swiss Light Source and the MAXIV synchrotron to measure beam sizes down to a few microns with submicron resolution.

Since synchrotron radiation is produced as the beam travels along an arc, there is a finite filament of emission that is specified by the field of view. Thus a single particle emitting OSR has a 'filament beam spread function' (FBSF) [6], rather than a SPF. The former can be calculated from theory or a simulation code, e.g. SRW [7].

Figure 4 (left) shows a line scan of Pi polarized OSR (488nm), fit to a convolution of the FBSF with a Gaussian beam distribution with $\sigma = 5\mu m$; (right) shows the sensitivity of the visibility to beam size. This curve indicates that beam size measurements $< 3\ \mu m$. may be possible with this method.

Note that the entire distribution is involved in the fit. This fitting procedure can produce much higher accuracy that a visibility measurement alone. This idea is also exemplified in the following topic.

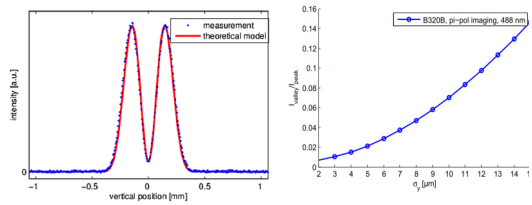

Figure 4: (left) Pi polarized OSR scan (black dots) and fit (red line) to FBSF convolved with a Gaussian beam distribution with; (right) visibility of Pi polarized OSR vs. beam size (from [6]).

High Resolution Scintillator Studies

In the last several years there has been a renaissance of interest in scintillators for beam imaging applications, especially to mitigate coherent OTR produced by beam micro bunching that is commonly observed in high brightness FELs. COTR is highly non linear with current density.

Systematic studies of the image resolution of various scintillator screens have recently been made using the MAMI accelerator [8]. The crystal scintillator LYSO has found to be the best of the materials measured for high-resolution imaging.

In addition, a line source model with isotropic emission has been developed for scintillators. ZOS is then used to do ray tracing of this source through the optics at the peak emission wavelength of the scintillator (420 nm), to produce a *single particle line spread function* (SPLF) that is qualitative similar to the FBSF discussed above. By convolving the SPLF with a 2D Gaussian model for the beam, the image data can be fit to find the vertical (y) and horizontal (x) beam sizes.

Figure 5 (left) shows the beam image observed from a scintillator inclined at 45^0 with respect to the beam direction; and (right) the best fit to a vertical line scan through the center of the beam image. Note the high resolution of the measured vertical beam size produced by the fit. Furthermore, simulations show that by using a thinner scintillator it may be even be possible to improve this resolution.

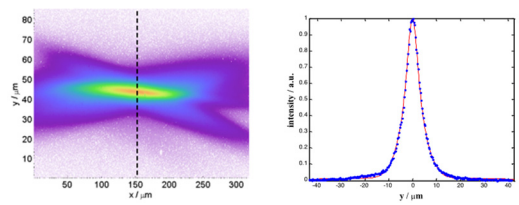

Figure 5: (left) image of the MAMI beam intercepting a 200 μm thick LYSO scintillator; (right) vertical line scan (dots) and fit to the data giving $\sigma_y = 1.44\,\mu m$ (from [8]).

ISBN: 978-3-95450-184-7 doi:10.18429/JACoW-IPAC2018-THXGBE2

HIGH DYNAMIC RANGE IMAGING

High dynamic range imaging (DR~10^6) is needed to study beam halo. A number of optical techniques to achieve high DR have been studied in recent years. These include: 1) the Lyot coronagraph adapted to beam measurements [9]; 2) optical emission produced by wire scanners; and 3) simultaneous imaging of OTR using cameras with different gains [10].

My colleagues and I have developed an HDR imaging system based on digital micro-mirror array (DMD). The latter is used to create a series of masks to block selected optical intensity levels within the beam image. The DR of each mask measurement is limited to the DR of the imaging camera used (typically 10^2-10^3). As the intensity threshold is decreased the exposure time is linearly increased to maintain approximately the same DR for each image. The procedure is followed until the mask size fills the area of the DMD. The images are then normalized by the exposure time and overlapped to create a *composite* HDR image [11].

Several important other limits to this process have been noted: 1) diffraction produced by the aperture of first lens of the imaging system; 2) the contributions of misalignments, scattering and aberrations of the optical elements of the system; 3) diffractive effect of the DMD micro mirrors themselves; and 4) diffraction from the boundary of the mask. The combined result is an 'effective point spread function', which can be measured with a sufficiently small laboratory point source. These limitations were partially addressed in previous studies [11] and it was shown that they did not limit the DR of our measurements.

Figure 6 shows normalized line scans of multiply masked OSR images of the JLAB ERL electron beam [12]. The inserted image shows the final mask and the halo surrounding this mask.

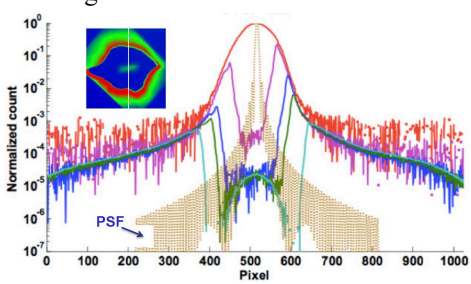

Figure 6: Composite vertical line scans of masked images created with a DMD; the calculated PSF of the optical system; and false color image of the halo surrounding the mask and 'diffracted' image of the beam core; from [12].

Note the inserted picture in the upper left hand corner, which shows a 'ghost' image of the beam present in the center of the masked region. This image is created by light diffracted by the edges of the micro-mirrors. The vertical profile of this beam image is the green line scan, which replicates the central region of the unmasked image scan in red, albeit with a peak amplitude 10^5 smaller than the peak of the unmasked image. Also note that the PSF due to diffraction from the primary objective lens (calculated in this case from diffraction theory), is well below the data scan curves indicating that the wings of the PSF do not limit the measured DR.

INTERFEROMETRIC METHODS

In this section I will discuss current advances in interferometry using different types of radiation that allow measurement of the rms beam size and the rms divergence generically denoted by σ and σ' respectively.

Diffraction Radiation

The first topic that I will discuss is the interference of optical diffraction radiation (ODR) from two longitudinally separated apertures.

Unlike OTR, far field angular distribution (AD) of ODR from a slit or other aperture is a function of the position and distribution of the beam with respect to the center of the aperture. In [13] it was shown for a horizontally aligned slit that the vertical offset of a single particle from the slit axis and a finite vertical beam size affects the AD in the same way. Therefore, in order to isolate the effect of beam size it is important to center the beam on axis. When this is done the angular distribution of ODR primarily depends on the rms vertical beam size and the rms divergence.

These two parameters can be separated by either rotating the slit 90^0 or by introducing a second slit longitudinally separated from the first [14]. In the former case the horizontal and vertical polarizations of the ODR can be used to separate out the effects of the corresponding rms beam sizes and divergences. The latter configuration has the advantage that the first slit acts like a mask that blocks any upstream radiation from contaminating the observed interference between forward ODR from the first slit and backward reflected ODR from the second slit, when both slits are inclined at 45^0 with respect to the beam axis.

If the distance between the slits is larger than the coherence length, i.e. $L > L_c \sim \gamma^2\lambda$, high frequency interference fringes will be observed modulated by the single slit ODR angular distribution pattern. The visibility of these interferences will only depend on σ'. However, because of the strong dependence of the coherence length on beam energy, this scheme is practically limited to beam energies E < 1 GeV. If on the contrary $L < L_c$, the interference pattern is more complicated and the effects of σ and σ' are mixed. Nevertheless, a method has been devised to separate them by using slits with different widths and a small ($50\,\mu m$) vertical offset of the second slit from the axis of the first that is enough to break the symmetry between the two effects [15]. The advantage of this scheme is that the ODR interferometer is very compact. However, the device must be precisely made and characterized, and the analysis and fitting of the data obtained by this technique is complex.

Figure 7 (left) shows ODR interferences (ODRI) from two *non-collinear* slits and the effect of σ and σ' on the

ISBN: 978-3-95450-184-7 doi:10.18429/JACoW-IPAC2018-THXGBE2

observed interferences. The two effects are now distinguishable and a multi-parameter fit of the data can extract both quantities; (right) shows a scan of the inferred beam size measured as a function of current in the quadrupole magnet that controls its focusing power. The emittances obtained by fitting the OTR and ODRI beam size data to the envelope equation agree within experimental error.

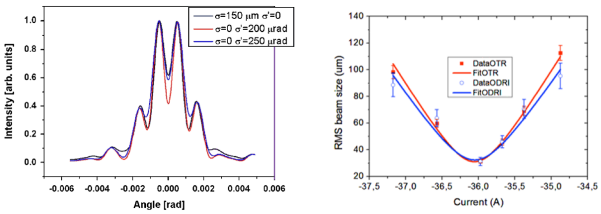

Figure 7: (left): Comparison of the effect of beam size and divergence on ODRI; right: comparison of quad scans using beam size obtained with ODRI and OTR.

A similar two-slit ODRI system has been developed for use at KEK [16]. However, because of the very low emittance of the ATF2 beam, the effect of divergence on the ODRI is negligible. This greatly simplifies the analysis of the data. In this case the visibility of the ODRI pattern, i.e. the ratio of the peak intensity to that of the central minimum can be used directly to measure the rms beam size. The resolution of this method has recently been improved by observing UV DRI [17].

Optical Synchrotron Radiation

Measurements of first order optical coherence function from the interference of OSR from two transversely separated pinholes (Young's method) is a well developed beam size diagnostic method that has been successfully used at many accelerators [18].

Recently, the technique has been extended by use of scanning a multi-element aperture, i.e. a 'diffraction object' across the OSR beam at the SLS and MAXIV synchrotrons and used to measure beam sizes $< 5\ \mu m$. Simulations have shown that this number can be improved to $< 3\ \mu m$ using the UV component of the SR [6].

In addition, a rotating pinhole OSR interferometer has been developed, that measures the beam size projected along the axis passing through the pinholes as a function of rotation angle [19]. This system has been used to measure the size of elliptically shaped beams that are typically observed at synchrotrons. Multiply projections allow a 2D reconstruction of the beam's shape with low error using a relatively small number of angles. Studies also show that beam sizes smaller than the lower limit of any one axial measurement can be obtained. This is accomplished by a fit of the data to the theoretical curve that relates the projected beam along the axis of the OSRI pinholes to the inclination angle of the semi-major axis of the ellipse.

EMITTANCE - INTENSE BEAMS

Modified Quad Scan Method

My colleagues at the Cockcroft Institute, the University of Maryland and Argonne National Laboratory (ANL) and I are developing a novel method to determine the RMS emittance of high intensity (i.e. space charged dominated) beams. The technique employs a method to compute the correlation term in the equation for the RMS geometrical x and y emittances in terms of the correspondingly measured rms divergence and beam size [20]. It is possible to measure both of these observables simultaneously, e.g. using OTR [21], OSR [22] and as we have just discussed ODR [15].

The algorithm to determine the emittance uses the beam envelope equation in reverse and the correlation term as a control variable. The latter is iterated until the rms beam size and divergence predicted by the envelope equation at the focusing magnet match the values measured at a downstream screen. The method requires a minimum of two pairs of measurements at two values of focusing strength. Thus a complete quad scan such as measured in Figure 7 is not required to produce the rms emittance. Moreover, the method works equally well for emittance or space charge dominated beams.

Proof of principle experiments are now underway at ANL's Advanced Wakefield Accelerator (AWA) to validate this new technique. Phase space tomography (PST) measurements have already been performed to provide a benchmark emittance value; and OPAL simulations have been done to predict the rms emittances as well as the range of beam divergences and sizes where the emittance is constant. The PST measurements and simulations are in agreement and produce a horizontal rms emittance of 8.4 microns, which we expect to duplicate with the new method in the very near future.

Optical Phase Space Mapping

D. Rule and I originally developed the concept of optical phase space mapping (OPSM), the optical equivalent of the pepper pot technique [23] and successful proof of principle experiments were performed [24,25]. It was shown [24] that even a small number of samples (two) of beam divergence and trajectory angle values is sufficient to provide an estimate of the tilt angle and the parameters of the beam ellipse. From these, an improved measurement of the rms emittance can be made.

The data for OPSM is acquired by using an optical mask that has one or more pinholes placed in the image plane of a beam imaging system. The light (OTR in our studies) emerging from each pinhole is observed in the focal plane of a lens. The AD of the OTR seen in this plane from each pinhole is analysed to produce the local value of the rms divergence and trajectory angle. This data acquired at a number of sampling points within the beam image is used to create a trace space plot of the beam. This method is completely analogous to the standard pepper-pot technique.

ISBN: 978-3-95450-184-7 doi:10.18429/JACoW-IPAC2018-THXGBE2

The advantages of this technique are: 1) the system is all optical; no beam collimation system is required; 2) the measurements sample the phase space at a single longitudinal position along the beam line; hence there is no possibility of phase space distortion in the drift region between the collimator and the imager, as can be the case for the common pepper-pot collimator method; and 3) in principle, by using a multiple aperture mask and a sufficiently sensitive imaging detector, the sampling can be done on a single shot.

Two new developments have recently come about to advance this technique and make it more practical for beam diagnostics applications: 1) a scheme that I have developed to do OPSM electronically using a DMD to create and manipulate the optical mask; and 2) a method that INFN LNF has independently developed to perform OPSM using a micro-lens array [26].

Figure 8 shows a schematic of the DMD based system. This shows how any beam radiation source can be used to image the beam and to measure the divergence and trajectory angle from an electronically generated pinhole mask on the DMD. However, the DMD can be programmed to produce an arbitrary fixed or movable mask, e.g. an array of pinholes.

The effects of mask size and shape on the resolution of the imaging system are currently being studied experimentally using the laser point source mentioned above and via Zemax simulations.

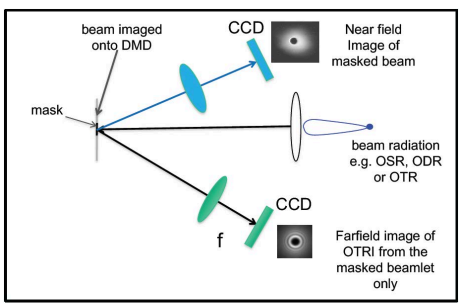

Figure 8: OPSM with a DMD.

The method developed by INFN LNF uses single foil OTR to image the beam onto a micro-lens array. The OTR ADs from a number of points within the image are observed in the common focal plane of the micro-lenses. The visibility of each AD is then used to measure the local rms divergence at a number of micro-lens positions [26]. It has been demonstrated that this method can measure the rms divergence of a 125 MeV electron beam at several points within the beam on a single shot. The chief limitation of this technique is the measurable visibility of the observed single foil OTR AD, which is $\sim 0.1\,\gamma^{-1}$. This restricts the range of divergences that can be measured for a given beam energy.

NOVEL BUNCH LENGTH MONITOR

Dispersive and Fourier transform spectroscopy of coherent beam associated radiation, e.g. CTR, CDR and CSR, are both commonly used to measure the spectrum, longitudinal bunch form factor and rms bunch length. With the aid of various phase retrieval algorithms, the bunch shape can also be inferred using these methods.

My colleagues and I have taken a different approach to measure the rms bunch length. This method uses the frequency integrated *angular and spatial distributions* (i.e. the far field and source field images, respectively, of coherent radiation produced by the bunch). We have concentrated in particular on CDR because of its versatility and non-invasive nature, but other types of coherent radiation can be similarly employed. The theory behind the method is explained in [27].

The advantages of this approach are: 1) a relatively small band width detection is needed; 2) the measurement apparatus is modest, i.e. a simple imaging system and single element scanning detector or imaging array; and 3) retrieval of the bunch length from the data is straight forward; 4) the method is non-invasive; 5) the method is applicable to a wide range of bunch lengths (mm – sub micron); and 5) in principle, the measurement can be made on a single shot.

A proof of principle experiment that imaged the AD of CDR was performed some time ago [28]. The bunch lengths obtained from the AD measurement compared to very well (with 10%) to those obtained with electro-optic sampling.

More recently we have investigated the use of the *spatial distribution,* rather than the AD, of CDR to do bunch length measurements, because the former is less sensitive to interference from upstream sources. A preliminary experiment to test this concept was done at SLAC-FACET that qualitatively showed that the predicted spatial distribution [29]. But because of the shutdown of FACET we were not able to quantitatively verify the results. In lieu of this, we are presently preparing follow-up experiments at the Swiss FEL and/or MAXIV to validate this new method.

Figure 9 shows the predicted spatial distributions of CDR for three bunch lengths that are expected to be observed at the Swiss FEL, right after the first bunch compressor at a beam energy of 330 MeV. The imaging optics and detection system for this experiment have been built, tested and are ready for installation [30]. Note that the rms beam size at PSI is about 100 μm, which is much smaller than the width of the predicted CDR distributions. This means that the single particle SPF of the radiation will be observed.

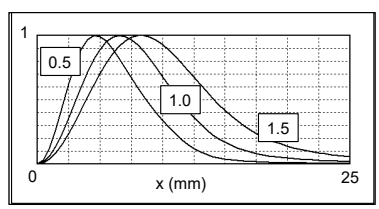

Figure 9: Normalized CDR spatial distributions for three bunch lengths: 0.5, 1.0 and 1.5 picoseconds (rms) predicted for the Swiss FEL at 330 MeV; relative peak amplitudes: 4.5, 0.5 and 0.09 respectively.

ISBN: 978-3-95450-184-7 doi:10.18429/JACoW-IPAC2018-THXGBE2

CONCLUSIONS

I have reviewed progress in the development of a number of optically based beam diagnostic methods that overcome the limitations of what was previously considered to be possible, by the use of modern optical methods. These include the use of the single particle source function (SPF), to measure sizes well below the diffraction limit; very high dynamic range imaging; optical phase space mapping; and the use of interferences of transversely and longitudinally separated beam associated radiation sources to measure very small values of beam size, divergence, emittance and bunch length. Many of these same methods can also be applied to the measurement of energy spread, e.g. the beam size in a magnetically dispersive region is correlated with the energy spread.

The development and application of novel optical methods to measure 'extreme' beams, with increasingly smaller emittances and bunch lengths, continues to advance at a rapid pace. We can expect this trend to continue well into the future.

ACKNOWLEDGEMENTS

I would like to thank the many colleagues, who have scientifically contributed to the research results presented here and generously provided material for the preparation of this review paper. They are J. Wolfenden, H. Zhang and C. Welsch, University of Liverpool/ Cockcroft Institute; T. Pacey, University of Manchester/ Cockcroft Institute; D. Walsh, M. Surman, R. Smith, STFC ASTEC/ Cockcroft Institute; A. Shkvarunets, University of Maryland; R. Ischebeck, G. Orlandi, F. Frei, N. Hiller, S. Bettoni, and V. Schlott, Paul Scherrer Institut (SwissFEL); J. Power, M. Conde, N. Nevue, Argonne National Lab (AWA); C. Clarke, A. Fisher, SLAC (FACET), J. Corbett, SLAC (SPEAR3); A. Aryshev, T. Mitsuhashi, N. Terunuma, KEK (ATF2); P. Karataev, K. Kruchinin, RHUL/John Adams Institute; M. Bergamaschi, T. Lefevre, S. Mazzoni, R. Kieffer, CERN; A. Andersson, MAXIV; A. Cianchi, E. Chiadroni, F. Bisesto, INFN (LNF); G. Kube, DESY; and L. Torino, U. Ariso , ALBA.

REFERENCES

[1] D. Xiang and W. H. Huang, Nuc. Instrum. and Methods A, 570, 357–364 (2007).

[2] B. Bolzon, et. al., PRAB, 18, 082803 (2015); and references therein.

[3] L. Sukhikh, G. Kube and A. P. Potylitsyn, PRAB 20, 032802 (2017).

[4] K. Kruchinin et al., J. Phys. Conf. Ser. 517, 012011(2014).

[5] J. Wolfenden, R. Fiorito and C. Welsch, " Energy Independence in Optical Transition Radiation Imaging", paper WEPAF036, this conference.

[6] A. Andersson, "Emittance Measurements on Future Ring Light Sources", Proc. of the 60th ICFA Advanced Beam Dynamics Workshop, *FLS2018*, Shanghai, Mar 5-9, 2018.

[7] O. Chubar and P. Elleaume, "Accurate and efficient computation of synchrotron radiation in the near field region", Proc. of EPAC1988 Stockholm, SE, p. 1777.

[8] G. Kube, S. Bajt, A. Potylitsin, et. al. "High Resolution Scintillator Studies", Proc. of IBIC15, Melbourne (2015).

[9] T. Mitsuhashi, "Design and Construction of Coronagraph to Observe Beam Halo", Proc. of EPAC2004, Lucerne, SZ.

[10] P. Evtushenko," Large Dynamic Range Beam Diagnostics for High Average Current Electron Linacs", Proc. of IPAC14, Dresden, DE (2014).

[11] H. Zhang, R. Fiorito, A. Shvarunets and C. P. Welsch, PRAB 15, 072803 (2012); J. Egberts, C.P. Welsch, JINST 5, P04010 (2010).

[12] R. Fiorito, A. Shkvarunets, H. Zhang, et. al. "Optical Synchrotron Radiation Beam Imaging with a Digital Mask", Proc. of BIW12, Newport News, VA, 2012.

[13] M. Castellano, Nuc. Instrum. and Methods A, 394, 3, 275 (1997).

[14] R. Fiorito and D. Rule, Nuc. Instrum. and Methods B, 173, 67-82, (2001).

[15] A. Cianchi, et. al., New Journal of Physics, 16.11 (2014); and PRAB, 14, 102803 (2011).

[16] R. Kieffer, et. al., Nuc. Instrum. and Methods B, 402, 88 (2017).

[17] M. Bergamaschi, "DR Measurements at ATF2", Proc. of CLIC Workshop, CERN, Geneva, January 23, 2018.

[18] T. Mitsuhashi, "Recent Trends in Beam Size Measurement Using the Spatial Coherence of Visible Synchrotron Radiation", Proc. of IPAC15, Richmond, VA (2015).

[19] L. Torino and U. Ariso, PRAB, 19, 122801 (2016).

[20] K. Poorrezaie, R. Fiorito, et. al., PRAB 16, 082801(2013).

[21] M. Holloway, R. Fiorito, A. Shkvarunets, et. al., PRAB 11, 082801 (2008).

[22] R. Fiorito, A. Shkvarunets, D. Castronovo, et. al., PRAB, 17, 122803 (2014)

[23] R. Fiorito and D. Rule, US Patent No. 5120968, 1992.

[24] G. LeSage, T. Cowan, R. Fiorito and D. Rule, PRAB, 2(12),122082 (1999); and PRAB **5**, 059901 (2002).

[25] R. Fiorito, A. Shkvarunets and P. O'Shea, "Optical method for mapping the transverse phase space of a charged particle beam", p.187, AIP CP648, BIW(2002).

[26] A. Cianchi, et. al. Nuc. Instrum. and Method A (2017).

[27] A. Shkvarunets and R. Fiorito, PRAB 11, 012801 (2008).

[28] A. Shkvarunets, R. Fiorito, F. Mueller and V. Schlott, "Diagnostics of the Waveform of Picosecond Electron Bunches Using the Angular Distribution of Coherent Submillimeter Transition and Diffraction Radiation", Proc. of DIPAC07, Venice, IT (2007).

[29] R. Fiorito, C. Welsch H. Zhang and A. Shkvarunets, "Novel Single Shot Bunch Length Diagnostic using Coherent Diffraction Radiation", Proc. IPAC15, Richmond, VA (2015).

[30] J. Wolfenden, R. Fiorito, T. Pacey, C. Welsch and A. Shkvarunets, "Coherent Diffraction Radiation Imaging as a RMS Bunch Length Monitor", paper WEPAF035, this conference.